DATA ANALYSIS TECHNIQUES FOR THE ACTS MOBILE EXPERIMENTS

E. Satorius and D. Pinck

Jet Propulsion Laboratory, California Institute of Technology, Pasadena, California

Abstract JPL has developed a K-/Ka-band mobile terminal and is currently conducting a series of mobile experiments to explore the potential of K-/Ka-band to meet the needs of future mobile satellite services. In support of the AMT field experiments, data analysis software algorithms have been developed for processing the various data received at the fixed and mobile terminals. This processing consists of both quick-look analysis of events recorded at a single terminal as well as in-depth analysis of data events collected from both terminals. In this paper, we provided an overview of these data analysis techniques and provide some examples.

L Introduction

JPL has developed a proof-of-concept breadboard mobile terminal system to operate in conjunction with ACTS at Ka-band [1]. As depicted in Figure 1, this system comprises a bent pipe propagation link connecting terminals at fixed and mobile sites. The terminals are identical although only a single pilot signal, from the fixed to the mobile station, is used to aid in Doppler compensation and mobile antenna tracking. Furthermore, ACTS possesses the high-gain spot-beam antennas required to support small mobile and personal terminals. The resulting ACTS Mobile Terminal (AMT) breadboard system will support both voice and data links and will be demonstrated in typical mobile and stationary environments. Basic technologies that enable Ka-band communications will be demonstrated first, followed by various enhancements to achieve improved system performance and efficiency.

The research described in this paper was carried out by the Jet Propulsion Laboratory, California Institute of Technology, under contract to the National Aeronautics and Space Administration,

Key features of the AMT system (see [1]) include an adaptive fade compensation algorithm (AFCA) to help overcome Ka-band propagation impairments (i.e., rain attenuation) by adaptively changing the data rate. In addition, adaptive power control is being used between the ground station and ACTS to compensate for uplink propagation path attenuation. The AMT utilizes Differential Binary Phase Shift Keying (DBPSK) modulation with rectangular pulse shaping to provide resistance against the expected ACTS' phase noise characteristics. To accommodate the large Doppler shifts and other frequency offsets, which can especially degrade system performance at the lower data rates, an innovative Doppler estimation and correction algorithm has been developed for the AMT. This algorithm is based on an open-loop, delay-and-multiply architecture and can accommodate Doppler shifts well in excess of the symbol rate. Finally, the high-gain AMT antenna system is being designed to provide for accurate satellite-tracking as well as good cross-polarization isolation, In this way, AMT will demonstrate a viable Ka-band communication system that realizes the advantages higher frequency communication bands can offer.

In support of the AMT field experiments, data analysis software algorithms have been developed for processing the various data received at the fixed and mobile terminals. This processing is carried out both by the Data Acquisition System (DAS) as well as a Sun Spare 10 workstation, The DAS serves several purposes: (i) data reduction, (ii) "quick-look" data analysis and display and (iii) data recording for post-test data analysis by the Sun workstation. The primary purpose of the workstation is in-depth analysis of data events collected from both the fixed and mobile

terminals. In the remainder of this paper, we first describe in Section II the basic quick-look data analysis performed by the DAS followed in Section 111 by the more in-depth analysis techniques implemented on the Sun workstation.

11. Quick-Look Data Analysis

The primary goals of the DAS quick-look anal ysis are to: (1) verify functionality of the AMT design, (2) characterize the Ka-band mobile channel and (3) act as a debugging tool during experimentation. In achieving these goals, we make use of the various input data summarized in Table 1. This table comprises the sources of the input data, i.e., the subsystems which generate the data as well as descriptions of the data types and the relevant AMT functional requirements.

To verify the basic AMT functionality, a combination of real time data analysis algorithms and displays are used, Consider first the antenna controller subsystem wherein azimuth pointing data is used to verify that its functional requirements are met. This is done via display and statistical analysis of the pointing data. First, the pointing data are displayed by the DAS to provide qualitative assessment of the antenna controller subsystem performance. In addition, an estimate of acquisition time can be obtained from such a display as well as tracking performance, especially when combined with the environmental data, i.e., the vehicle position, velocity and heading information. This latter information is used to compute the expected antenna pointing angle, ϕ_{env}, from:

$$\phi_{env} = \pi + \tan^{-1}\left\{\frac{long + 100^{\circ}}{lat}\right\} - heading,$$

where *lat, long, heading* denote the latitude, longitude and heading of the vehicle, respectively. Simultaneous displays of the azimuth pointing angle data and ϕ_{env} can then be used to verify the antenna tracking requirement, Other analyses of the antenna pointing angle data include sample mean and variance calculations as well as histogram analysis. These statistical analyses are also used to verify the antenna functional requirements.

Quick-look analyses of the pilot demodulator subsystem data consists of first displaying the instantaneous pilot power:

$$Pi = I_i^2 + Q_i^2,$$

where Ii a n d Q_i denote the in-phase and quadrature components of the complex demodulated pilot signal out of the pilot phase locked loop (PLL). In addition, the pilot power data, P_i^{nc}, from the noncoherent pilot power detector, is also displayed. Generally, *Pi* and P_i^{nc} will be different due to the different bandwidths used in the pilot PLL demodulator and the noncoherent pilot power detector. Visual inspection of these displays, in combination with the pilot PLL lock indicator, provides a qualitative assessment of pilot demodulator subsystem performance. Furthermore these displays can be used to estimate the PLL acquisition time and thus verify the corresponding functional requirement.

Spectral analyses of the complex demodulated pilot data and the noncoherent pilot power data are also carried out to aid in estimating received pilot level as well as received pilot carrier-to-noise power ratio (CNR). This information, in turn, is used to verify the pilot acquisition and tracking subsystem requirements (Table 1). As a further means to verify the pilot subsystem functional requirements, the estimated Doppler offset, Af, based solely on environmental data, is computed from:

$$\mathrm{Af} = v_{veh} \cdot \cos(\theta_{el}) . \cos(\phi_{env}) . f_{rec} \;/\; c,$$

where v_{veh} is the vehicle speed, f_{rec} *is* the received frequency, θ_{el} is the elevation angle from the vehicle to the satellite, ϕ_{env} is the expected antenna pointing angle as computed above and c is the speed of light. Frequency

tracking errors can then be assessed by comparing the PLL lock indicator data with the estimated Doppler offset, Δf. An example is depicted in Figure 2. As indicated, we would expect to lose PLL lock during periods when the estimated Doppler rate is largest, This information can also be used to verify the Doppler tracking rate requirement, i.e., by computing the time derivative of Δf and comparing it with the PLL lock indicator status.

Statistical analyses of the complex demodulated pilot data include computing the pilot power probability density, the cumulative fade distribution and fade distribution statistics, This information can be used to characterize the Ka-band mobile channel, i.e., in terms of the presence and severity of rain attenuation as well as the extent to which diffuse scattering is present. The latter is facilitated by extraction of the Rician parameter from the pilot power probability density. Additionally, the average distance of shadowing-based fades can be determined from the fade duration statistics simply by converting the fade duration (sees) into distance traveled by the vehicle. This is particularly important in characterizing the Ka-band mobile channel.

Further characterization of the channel can be obtained directly from the beacon attenuation data which are available at the fixed terminal via the beacon measurement subsystem (BMS) [2]. Statistical analysis of this data, identical to that described above for the pilot data, can be carried out to further characterize the Ka-band mobile channel. Additionally, due to the availability of beacon attenuation data at both 20 and 27 GHz, an assessment of frequency scaling laws for rain attenuation can be carried out, e.g., via scatter distribution analysis [3]. These attenuation data are also useful for evaluating the performance of the AMT AFCA [4].

Quick-look analysis of the data demodulator output provides verification of the basic modem performance. Specifically with reference to Table 1, it is seen that total modem losses arising from implementation, Doppler tracking errors and ACTS phase noise should be maintained to 3 dB, or less. This leads to a requirement that the measured bit error rate (BER) be 10^{-3}, or lower, at a bit energy-to-noise spectral density ratio, $E_b / N_0 = 9\ dB$.

To assess these requirements, it is essential that well controlled, accurate BER versus E_b / N_0 performance curves be obtained, To this end, we obtain measurements of E_b / N_0 directly from the data channel as follows. First, an average noise level, N_{avg} (dBm), from both before and after a data test transmission is computed from:

$$N_{avg} = \frac{1}{N_{cnt}} \sum_{i=1}^{N_{cnt}} N_i ,$$

where N_i are the noise samples (dBm) from the digital power meter and N_{cnt} denotes the number of noise samples. Similarly, the average signal plus noise level, S_{avg}, is computed from:

$$S_{avg} = \frac{1}{S_{cnt}} \sum_{i=1}^{S_{cnt}} S_i ,$$

where S_i are the signal plus noise data samples (dBm) from the digital power meter and S_{cnt} denotes the number of signal plus noise data samples. The received signal-to-noise ratio (SNR) is then computed from:

$$SNR\ (dB) = 10 \log_{10} \{ 10^{(S_{avg} - N_{avg})/10} - 1 \} ,$$

and E_b / NO is computed from:

$$E_b / No\ (dB) = SNR + 10 \log_{10} \left\{ \frac{B_N}{R_b} \right\} ,$$

where R_b is the data rate (kbps) and B_N is the noise equivalent bandwidth of the filter used in the digital power meter to measure N_i (B_N = 135 kHz).

Additionally, during data test transmissions, BER measurements are derived

from test data packets transmitted across the link, The following data are tallied between the start and end of a BER test: the total number of packets received (*PKTS*) and the total number of bit errors (*BITERR*). The *BER* are then computed from:

$$BER = \frac{BITERR}{NBPP \cdot PKTS},$$

where *NBPP* denotes the number of bits per packet. These data are combined with the measurements of E_b/NO to produce the BER versus E_b/NO performance curves that, in turn, are used to assess the data demodulator subsystem requirements,

HI. In-Depth Data Analysis Techniques

The Spare workstation data analysis software is broadly divided into three categories as depicted in Figure 3: statistical, display and prototype testing. The first two provide performance and diagnostic analyses of the baseline AFCA and protocol [5], whereas the latter provides information that will be useful in designing future systems. In particular, the statistical analysis software will include the computation of various fade and fade duration statistics (from pilot power and beacon data at the mobile terminal and fixed terminal, respectively) as well as the joint fade statistics, i.e., trajectories in the 2-D fade plane. In addition, the statistical analysis software will provide a quantitative indication of how well the baseline AFCA and protocol system performs by correlating various quantities.

The primary purpose of these techniques is to provide an in-depth analysis of data events collected from both the fixed and mobile terminals. Generally these techniques are used to evaluate the performance of both the AMT protocol and AFCA. Additionally they are useful in further characterizing the Ka-band mobile channel. As an example, 2D fade planes can be created by displaying uplink and downlink attenuation in a 2D (scatter plot) format. In particular, two different fade planes can be created corresponding to: (1) the uplink (~) and downlink (AL) attenuations over the forward path (fixed terminal-to-ACTS-to-mobile terminal) and (2) the uplink (AL) and downlink (AL) attenuations over the reverse path (mobile terminal-to-ACTS-to-fixed terminal). These attenuation data are derived either from the noncoherent pilot power data received at the mobile terminal, A_{do}^{f}, A_{up}^{r} (as described in [5]) or directly from the received beacon data at the fixed terminal, A_{up}^{f}, A_{do}^{r}.

Example fade planes are illustrated in Figures 4 and 5, Superimposed on these figures are the calculated AFCA data rate change (DRC) boundaries from [5]. As is seen, both forward and reverse links are equally sensitive to rain attenuation in the mobile terminal/ACTS up- and down-links, i.e., A_{do}^{f} in the case of the forward link (horizontal axis in Figure 4) and A_{up}^{r} in the case of the return link (vertical axis in Figure 5). Even 1.5-2.5 dB attenuations in these critical links will result in a DRC (9.6-4,8 kbps). In contrast, both links are much less sensitive to rain attenuation in the fixed terminal/ACTS up- and downlinks. This is a consequence of the larger power budget and greater antenna gain available at the FT. Clearly, these types of displays provide a good indication of link utilization and system performance.

As discussed in [4], a variety of displays and statistical analyses are useful in assessing the performance of the AMT AFCA and protocol, For example, integrated displays of the various attenuation, protocol packet and data rate information provide for an effective means to diagnose the AFCA/protocol performance. An example is depicted in Figure 6[1] corresponding to a scenario wherein rain attenuation is present at the mobile site but is not present at the fixed terminal and the received data rate at both terminals is initially

[1] AMT packets, as depicted in Figure 6, consists of: embedded requests (ERQs); data rate changes (DRCs); data rate change identifiers (DRCIDs) and acknowledgments (ACKs). See [5] for details.

9.6 kbps. Once the pilot-inferred attenuation reaches a certain level, however, the AFCA at the mobile terminal should force a transmit data rate change (from 9.6 to 4.8 kbps). As is seen, this type of display, which illustrates the various transmit and receive time lines, is a very useful diagnostic tool.

In addition, simple statistical tests can be applied to verify that the AFCA/protocol is working properly. In [4], so-called score statistics are devised to assess the internal consistency of the AFCA. Similar tests are also devised in [4] to assess the internal consistency of the AMT protocol structure. All of these tests are currently being evaluated via field demonstration experiments.

IV. CONCLUSION

JPL has developed a K-/Ka-band mobile terminal and is currently conducting a series of mobile experiments to explore the potential of K-/Ka-band to meet the needs of future mobile satellite services. To verifys ystem performance and characterize the K-/Ka-band mobile channel, an extensive data analysis software has been developed for both quick-look and in-depth analysis. Through these experiments, it is hoped that AMT development and the availability of ACTS as an invaluable satellite of opportunity will lead to other experiments and demonstrations of advanced land mobile terminal hardware; maritime and aeronautical systems; hybrid satellite and land based networks, and, eventually, true personal microterminals.

References

[1] K, Dessouky and T. Jedrey, "The ACTS Mobile Terminal," SATCOM Quarterly, JPL, Pasadena, CA, No. 8, January 1993.

[2] C. Zaks, "ACTS NGS Beacon Measurement Subsystem, " JPL ACTS Propagation Workshop, Santa Monica, CA, November 1990.

[3] W. Stutzman, et, al., "Communications and Propagation Experiments Using the Olympus Spacecraft -- Report on the First Year of Data Collection, " JPL SATCOM Report 202, October 1991.

[4] E. Satorius and D. Pinck, "AMT Data Analysis Software Specifications," JPL document in preparation.

[5] E. Satorius, "Rain Compensation Algorithm for the ACTS Mobile Terminal System," JPL Internal Memorandum, September 15, 1992.

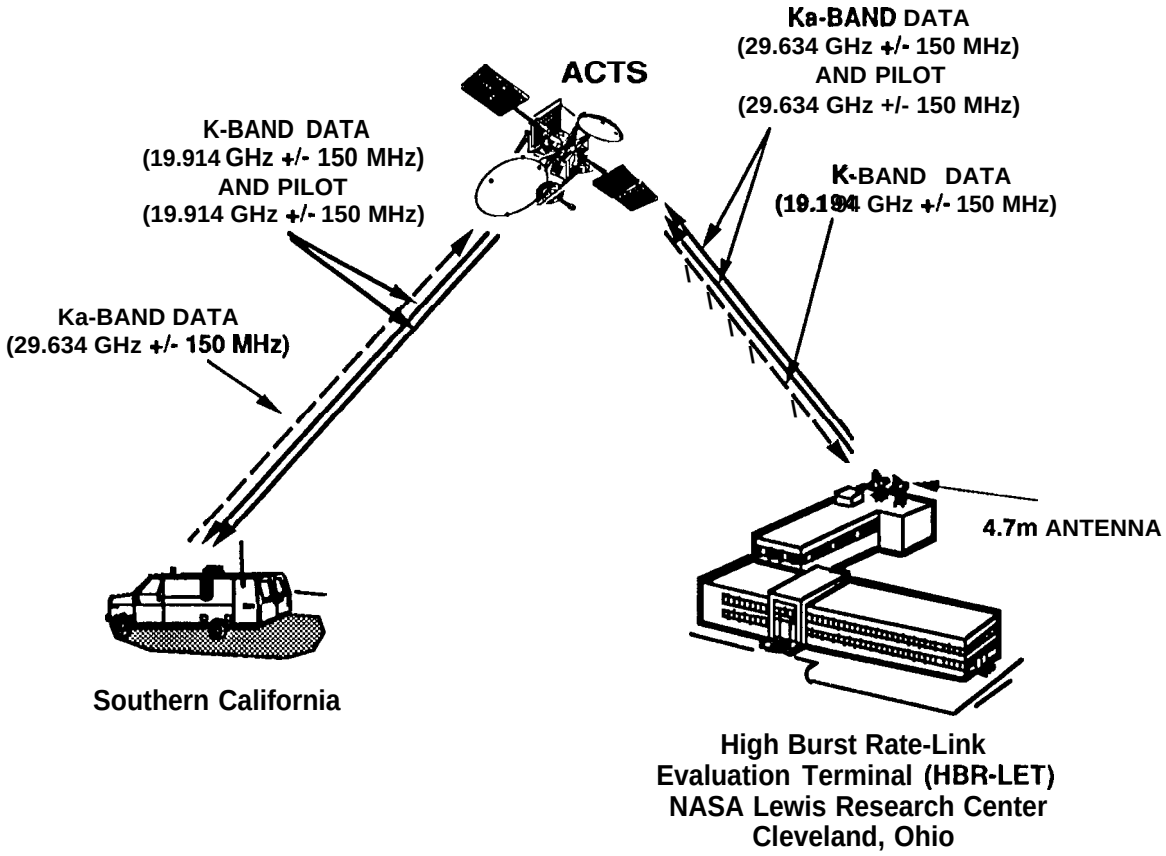

Figure 1, Proof-of-concept demonstration system for mobile Ka-band communications.

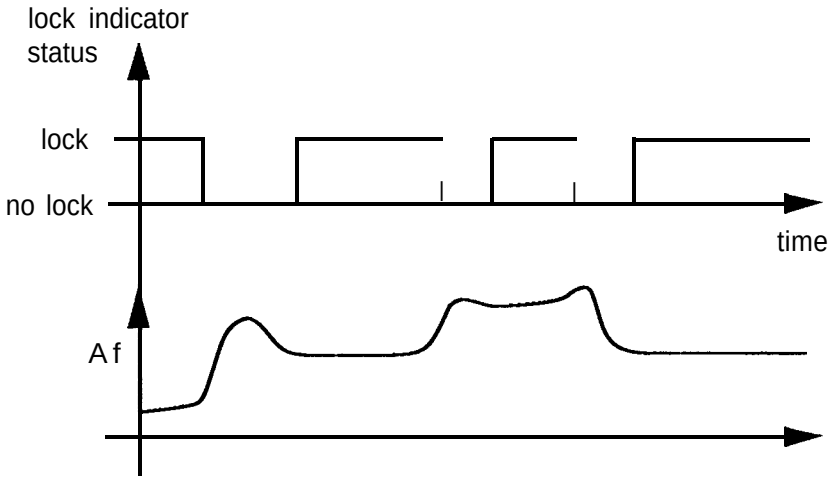

Figure 2. Sample time line display of PLL lock indicator status and estimated Doppler.

Source	Data type	Relevant AMT functional requirements
Antenna Controller	Antenna azimuth pointing angle	360" coverage acquisition time < 10 sec tracking rate to 45°/sec pointing error (@pilot CNR ≥ 50 dB-Hz): mean error< 0.2"; standard deviation < 0.8"
Pilot demodulator (Mobile terminal)	Complex demodulated output from PLL Pilot power data PLL lock status	Acquire and track pilot @ CNR ≥ 50 dB-Hz acquire pilot @ ± 4.5 kHz frequency offset and 250 Hz/sec rate acquisition time < 2 msec tracking phase jitter < 10"
Beacon attenuation data (Fixed terminal)	Attenuation data @ 20 and 27.5 GHz	N/A
Status information from the terminal controller	Transmit/receive bit rates Transmit/receive bit frequencies Transmit/receive powers Link type (voice, data, etc.)	NIA
Data from demodulator	Received data bits Noise/signal power	Digital implementation loss ≤ 1 dB @ 10^{-3} BER Max loss due to Doppler estimator errors ≤ 0.5 dB @ 10^{-3} BER ACTS phase noise degradation 1.5 dB @ 10^{-3} BER Total required Eb/No = 9 dB @ 10^{-3} BER
Environmental data	Vehicle position, velocity, heading	N/A

Table 1. Input data and basic AMT functional requirements.

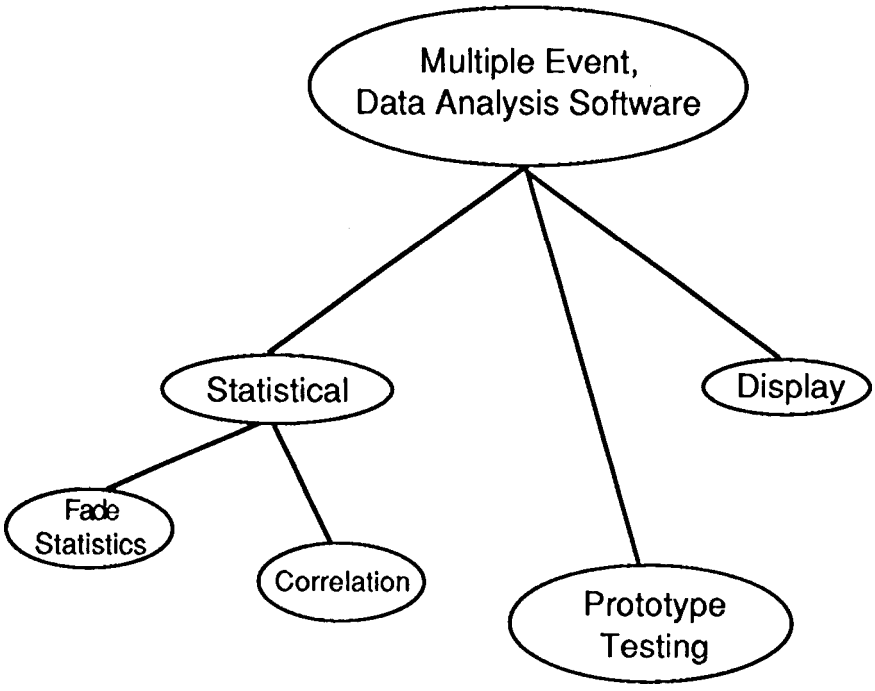

Figure 3. Spare workstation software organization.

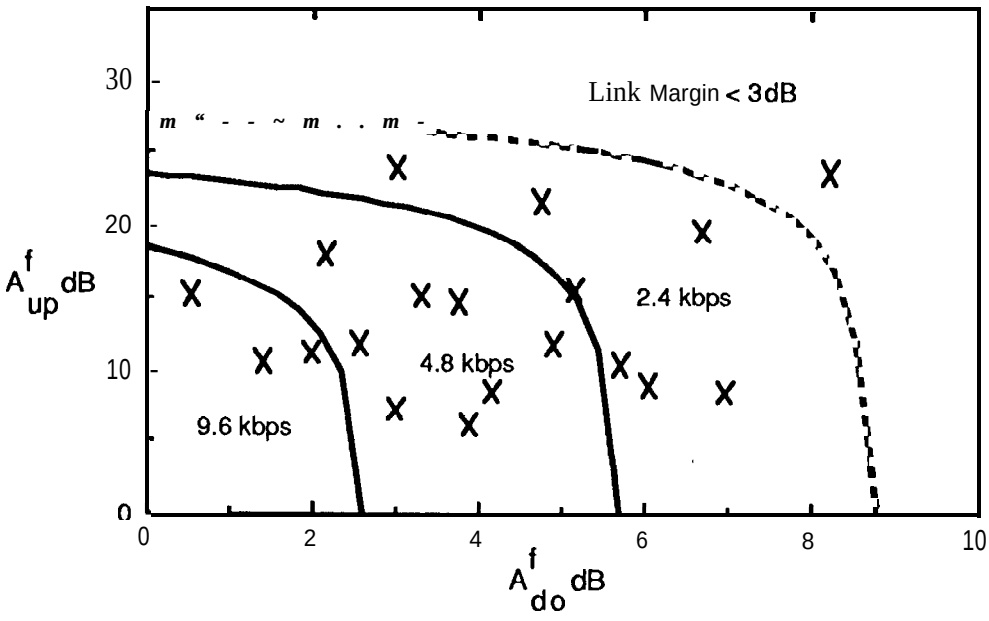

Figure 4. 2D fade planes with DRC boundaries for the forward link as a function of A^f_{up} and A^f_{do}. (X's denote sample data measurements,)

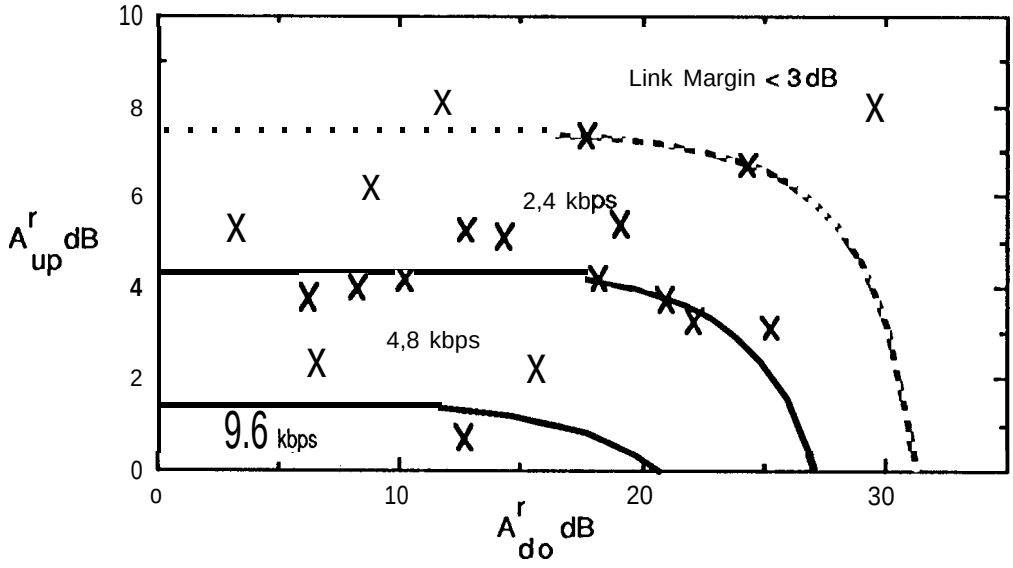

Figure 5. 2D fade planes with DRC boundaries for the reverse link as a function of A^r_{up} and A^r_{do}. (X's denote sample data measurements.)

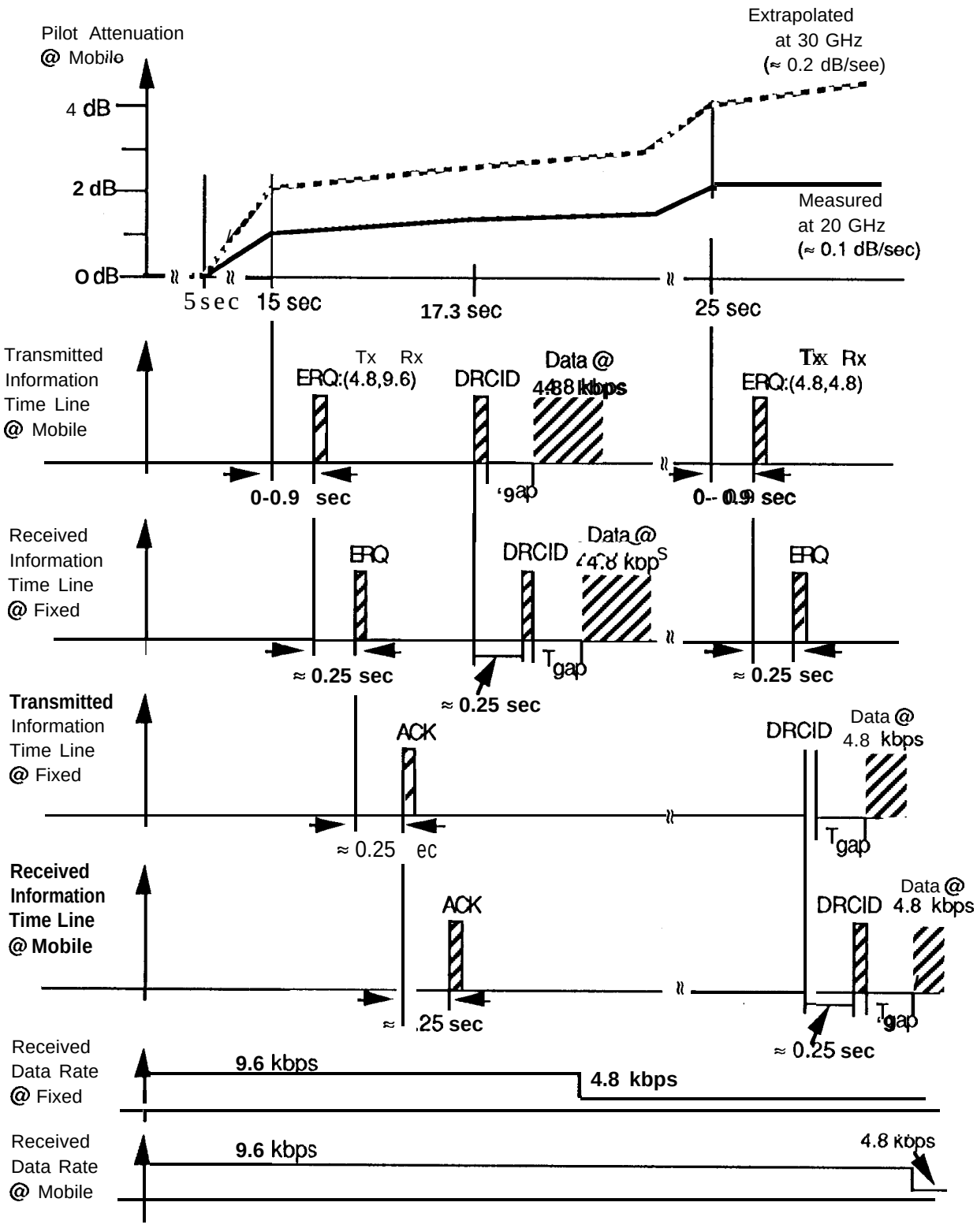

Figure 6. Sample integrated time-line display.